

Eigenmode Analysis of Optical Waveguides
by a Yee-Mesh-Based Imaginary-Distance
Propagation Method for an Arbitrary
Dielectric Interface

NUMATA, Satoshi / NAKANO, Hisamatsu / YAMAUCHI, Junji /
ANDO, Takashi / NAKAYAMA, Hiroki

(出版者 / Publisher)

IEEE

(雑誌名 / Journal or Publication Title)

Journal of lightwave technology / Journal of lightwave technology

(号 / Number)

8

(開始ページ / Start Page)

1627

(終了ページ / End Page)

1634

(発行年 / Year)

2002-08

Eigenmode Analysis of Optical Waveguides by a Yee-Mesh-Based Imaginary-Distance Propagation Method for an Arbitrary Dielectric Interface

Takashi Ando, *Student Member, IEEE*, Hiroki Nakayama, Satoshi Numata, Junji Yamauchi, *Member, IEEE*, and Hisamatsu Nakano, *Fellow, IEEE*

Abstract—A modified finite-difference (FD) formula for an arbitrary dielectric interface is applied to an imaginary-distance propagation method based on Yee's mesh. To confirm the validity of the modified method, we first analyze the eigenmode of a step-index circular fiber. A reduction in a discretization error is demonstrated in the evaluation of the field profile. Calculations of the normalized propagation constant show that the convergence rate of the modified FD formula is faster than that of traditional techniques and is comparable to that of a body-of-revolution technique. As a further application, we analyze the eigenmodes of sloped-side rib guides. These data agree well with previously published data.

Index Terms—Dielectric waveguides, electromagnetic fields, finite-difference methods, Maxwell equations, numerical analysis, optical waveguides.

I. INTRODUCTION

THE KNOWLEDGE of the eigenmode in an optical waveguide is of fundamental importance in the design of photonic integrated circuits. To date, many methods have been proposed for this important issue [1]–[4]. One of them is an imaginary-distance propagation method [2] based on Yee's mesh [4], [5]. The use of Yee's mesh has the advantage that the obtained eigenmode fields can directly be utilized for the finite-difference time-domain (FDTD) analysis [6].

In the FDTD method, the FD equations are conventionally obtained by discretizing Maxwell's equations with the use of a uniform orthogonal Yee mesh [7]. The space derivatives of Maxwell's equations are approximated by central-difference operators. It is well known that the conventional FD formula based on the central-difference operators induces a discretization error when a staircase approximation is introduced to describe an arbitrary dielectric interface.

To reduce the discretization error, researchers have developed some techniques [7]–[12]. One is the contour-path technique [7], [8], in which space cells local to a dielectric interface are deformed to conform with the interface position and the FD equations for the fields adjacent to the interface are derived on the basis of Faraday's and Ampere's laws. Unfortunately, the derived FD equations cannot naturally be incorpo-

rated into the imaginary-distance scheme. Another is the effective-dielectric-constant technique (EDCT) [7], [9]–[12], in which permittivities along the stepped edges of Yee's mesh are estimated by various averaging procedures. In contrast to the contour-path technique, the EDCT can be incorporated into the imaginary-distance scheme without difficulties [5].

Although the EDCT appears to improve the overall accuracy [9]–[13], the use of the conventional FD formula results in slow convergence as a function of transverse mesh size. This is because the conventional FD formula assumes the continuity of the field at a dielectric interface. In practice, the field and its derivative are often discontinuous at the interface. To exactly evaluate the field discontinuity, we have to take into account the boundary conditions.

Recently, a modified FD formula, which is constructed by combining the boundary conditions and one-sided difference operators, has been proposed for the FDTD algorithm [14]–[17]. It was demonstrated that the numerical errors caused by the traditional techniques are reduced in the analysis of scattering by a grating coupler [14] and by a dielectric cylinder [15]–[17]. However, no attempt has been made for the eigenmode analysis of an optical waveguide except for our preliminary report [18].

In this paper, we apply the modified FD formula [16], [17] to the imaginary-distance propagation method based on Yee's mesh and show the effectiveness of the modified method in the eigenmode analysis of an optical waveguide with an arbitrary dielectric interface. Furthermore, a body-of-revolution (BOR) [7] imaginary-distance propagation method is newly derived for a comparative study.

After the derivation of the modified and BOR methods, we first analyze a step-index circular fiber, since the exact field profile and propagation constant are available. Calculations of the field profiles show that the discretization error is substantially reduced by virtue of the modified FD formula. In the evaluation of the normalized propagation constant against transverse mesh size, the modified FD formula also achieves faster convergence than the staircase approximation and the typical EDCT [12]. It is worth mentioning that the results of the modified method almost coincide with those of the BOR method.

We next analyze the eigenmodes of sloped-side rib guides [19]. The evaluated effective indexes are in agreement with previously published data, including calculated and experimental results.

Manuscript received October 23, 2001; revised March 7, 2002.

The authors are with the Faculty of Engineering, Hosei University, Koganei, 184-8584 Tokyo, Japan.

Digital Object Identifier 10.1109/JLT.2002.800360

II. FORMULATION

A. Imaginary-Distance Propagation Method Based on Yee's Mesh

We summarize the formulation of the imaginary-distance propagation method based on Yee's mesh, following Lee's procedure [4]. Consider a linear lossless medium with permittivity ϵ and permeability μ . The formulation begins with Maxwell's equations

$$\nabla \times \mathcal{E} = -\mu \frac{\partial \mathcal{H}}{\partial t} \quad (1)$$

$$\nabla \times \mathcal{H} = \epsilon \frac{\partial \mathcal{E}}{\partial t} \quad (2)$$

where \mathcal{E} and \mathcal{H} are the electric- and magnetic-field vectors, respectively. \mathcal{E} and \mathcal{H} are normalized so that their magnitudes may be of the same order, i.e., $\mathcal{E} = \sqrt{\mu_0} \bar{\mathbf{E}}$ and $\mathcal{H} = \sqrt{\epsilon_0} \bar{\mathbf{H}}$. Substituting the set of normalized fields into (1) and (2), we get

$$\nabla \times \bar{\mathbf{E}} = -\frac{\mu_r}{c_0} \frac{\partial \bar{\mathbf{H}}}{\partial t} \quad (3)$$

$$\nabla \times \bar{\mathbf{H}} = \frac{\epsilon_r}{c_0} \frac{\partial \bar{\mathbf{E}}}{\partial t} \quad (4)$$

where $c_0 = 1/\sqrt{\epsilon_0 \mu_0}$ is the velocity of light in free space and ϵ_r and μ_r are the relative permittivity and permeability, respectively.

Let

$$\bar{\mathbf{E}}(x, y, z, t) = \mathbf{E}_{(x, y, z)} \exp[j(k_0 c_0 t - \beta_{\text{ref}} z)] \quad (5)$$

$$\bar{\mathbf{H}}(x, y, z, t) = \mathbf{H}_{(x, y, z)} \exp[j(k_0 c_0 t - \beta_{\text{ref}} z)] \quad (6)$$

where \mathbf{E} and \mathbf{H} are the slowly varying envelope functions of z , β_{ref} is the reference phase constant representing the fast-varying spatial phase, and k_0 is a wavenumber in free space. After substituting (5) and (6) into (3) and (4), and using a notation of $(x, y, z) = (k\Delta x, \ell\Delta y, m\Delta z)$, we obtain the following difference equations based on a uniform orthogonal Yee mesh:

$$\begin{aligned} E_{x, (k-1/2, \ell, m+1)} &= \frac{1}{1 - j\beta_{\text{ref}}\Delta z/2} \times [(1 + j\beta_{\text{ref}}\Delta z/2)E_{x, (k-1/2, \ell, m)} \\ &\quad + \Delta z\delta_x E_{z, (k-1/2, \ell, m+1/2)} \\ &\quad - jk_0\Delta z H_{y, (k-1/2, \ell, m+1/2)}] \end{aligned} \quad (7)$$

$$\begin{aligned} E_{y, (k, \ell-1/2, m+1)} &= \frac{1}{1 - j\beta_{\text{ref}}\Delta z/2} \times [(1 + j\beta_{\text{ref}}\Delta z/2)E_{y, (k, \ell-1/2, m)} \\ &\quad + \Delta z\delta_y E_{z, (k, \ell-1/2, m+1/2)} \\ &\quad + jk_0\Delta z H_{x, (k, \ell-1/2, m+1/2)}] \end{aligned} \quad (8)$$

$$\begin{aligned} H_{x, (k, \ell-1/2, m+1/2)} &= \frac{1}{1 - j\beta_{\text{ref}}\Delta z/2} \times [(1 + j\beta_{\text{ref}}\Delta z/2) \\ &\quad \times H_{x, (k, \ell-1/2, m-1/2)} \\ &\quad + \Delta z\delta_x H_{z, (k, \ell-1/2, m)} \\ &\quad + jk_0\Delta z \epsilon_r, (k, \ell-1/2) E_{y, (k, \ell-1/2, m)}] \end{aligned} \quad (9)$$

$$\begin{aligned} H_{y, (k-1/2, \ell, m+1/2)} &= \frac{1}{1 - j\beta_{\text{ref}}\Delta z/2} \times [(1 + j\beta_{\text{ref}}\Delta z/2) \\ &\quad \times H_{y, (k-1/2, \ell, m-1/2)} \\ &\quad + \Delta z\delta_y H_{z, (k-1/2, \ell, m)} \\ &\quad - jk_0\Delta z \epsilon_r, (k-1/2, \ell) E_{x, (k-1/2, \ell, m)}] \end{aligned} \quad (10)$$

$$\begin{aligned} E_{z, (k, \ell, m+1/2)} &= \frac{1}{(1 - j\beta_{\text{ref}}\Delta z/2)\epsilon_r, (k, \ell)} \times [(1 + j\beta_{\text{ref}}\Delta z/2)\epsilon_r, (k, \ell) \\ &\quad \times E_{z, (k, \ell, m-1/2)} - \Delta z\delta_x \\ &\quad \cdot \{\epsilon_r, (k, \ell) E_{x, (k, \ell, m)}\} \\ &\quad - \Delta z\delta_y \{\epsilon_r, (k, \ell) E_{y, (k, \ell, m)}\}] \end{aligned} \quad (11)$$

$$\begin{aligned} H_{z, (k-1/2, \ell-1/2, m+1)} &= \frac{1}{(1 - j\beta_{\text{ref}}\Delta z/2)} \times [(1 + j\beta_{\text{ref}}\Delta z/2) \\ &\quad \times H_{z, (k-1/2, \ell-1/2, m)} \\ &\quad - \Delta z\delta_x H_{x, (k-1/2, \ell-1/2, m+1/2)} \\ &\quad - \Delta z\delta_y H_{y, (k-1/2, \ell-1/2, m+1/2)}] \end{aligned} \quad (12)$$

where $\delta_\alpha \{\alpha = x \text{ or } y\}$ is a difference operator and μ_r is omitted due to a unit value. It should be noted that the E_z and H_z components are determined using the relations of $\nabla \cdot \epsilon_r \bar{\mathbf{E}} = 0$ and $\nabla \cdot \bar{\mathbf{H}} = 0$. As found in [4], the use of the divergence relations contributes to a reduction in roundoff errors with subsequent stability of the numerical results.

After changing the coordinate z in the propagation direction to $j\tau$ [2], we obtain the imaginary-distance scheme. The field distributions of all components are calculated stepwise in the $+\tau$ direction. An arbitrary input field that contains the lowest mode field converts into the lowest eigenmode field, as the input field propagates in the $+\tau$ direction. Note that the stability criterion of the scheme [4] is expressed as $\Delta\tau/\Delta_t < 1/\sqrt{2}$ for $\Delta_t = \Delta x = \Delta y$. If $\Delta\tau/\Delta_t$ is not within the stability criterion, the scheme becomes numerically unstable.

So far, $\delta_\alpha s$ in (7)–(12) have been approximated by the conventional central-difference operators. Hence, the field vectors across an arbitrary interface cannot be properly evaluated. To exactly evaluate the fields near the interface, we have to introduce the modified FD formula that takes into account the boundary conditions.

B. Modified FD Formula

The consecutive sampling points shown in Fig. 1 are considered. φ is the envelope function of any field component. Suppose that a dielectric interface between the core (ϵ_r, co) and cladding (ϵ_r, cl) is located between points $k-1/2$ and k and is at distance $\gamma_x \Delta x$ ($0 \leq \gamma_x \leq 0.5$) from point k . \mathbf{n} is a unit normal vector at the interface. Let $\varphi^{(1)}$ and $\varphi^{(2)}$ refer to the fields in the core and cladding around the interface, respectively. In this case, the modified FD formula is applied to $\delta_x \varphi_{k-1/2}$ and $\delta_x \varphi_k$.

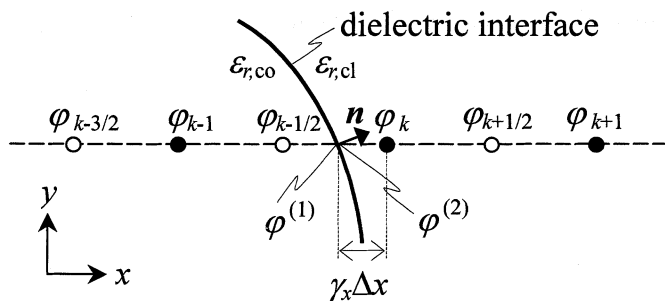


Fig. 1. Sampling points near a dielectric interface.

To obtain the modified FD formula regarding $\delta_x \varphi_{k-1/2}$, we express the fields φ_{k-1} and $\varphi^{(1)}$ using Taylor series expansions

$$\varphi_{k-1} = \varphi_{k-1/2} - \frac{\Delta x}{2} \delta_x \varphi_{k-1/2} + O(\Delta x^2) \quad (13)$$

$$\varphi^{(1)} = \varphi_{k-1/2} + \left(\frac{1}{2} - \gamma_x\right) \Delta x \delta_x \varphi_{k-1/2} + O(\Delta x^2). \quad (14)$$

By subtracting (14) from (13), we obtain the following FD expression based on the one-sided difference operator:

$$\delta_x \varphi_{k-1/2} = \frac{1}{1 - \gamma_x} \frac{\varphi^{(1)} - \varphi_{k-1}}{\Delta x}. \quad (15)$$

Similarly, an expression for $\delta_x \varphi_k$ becomes

$$\delta_x \varphi_k = \frac{2}{1 + 2\gamma_x} \frac{\varphi_{k+1/2} - \varphi^{(2)}}{\Delta x}. \quad (16)$$

$\varphi^{(1)}$ in (15) and $\varphi^{(2)}$ in (16) are calculated taking into account the boundary conditions [16], [17] as follows.

For example, $\delta_x \epsilon_r, (k, \ell) E_x, (k, \ell, m)$ in (11) is expressed as

$$\delta_x \epsilon_r, (k, \ell) E_x, (k, \ell, m) = \frac{2\epsilon_{r,cl}}{1 + 2\gamma_x} \frac{E_x, (k+1/2, \ell, m) - E_x^{(2)}}{\Delta x}. \quad (17)$$

The relation between $E_x^{(1)}$ and $E_x^{(2)}$ at the interface is given by the boundary conditions of $\mathbf{n} \times \mathbf{E}^{(1)} = \mathbf{n} \times \mathbf{E}^{(2)}$ and $\mathbf{n} \cdot \epsilon_{r,co} \mathbf{E}^{(1)} = \mathbf{n} \cdot \epsilon_{r,cl} \mathbf{E}^{(2)}$, i.e.,

$$n_x E_y^{(1)} - n_y E_x^{(1)} = n_x E_y^{(2)} - n_y E_x^{(2)} \quad (18)$$

$$\epsilon_{r,co} (n_x E_x^{(1)} + n_y E_y^{(1)}) = \epsilon_{r,cl} (n_x E_x^{(2)} + n_y E_y^{(2)}). \quad (19)$$

By eliminating $E_y^{(1)}$ from (18) and (19), we can write $E_x^{(2)}$ as

$$E_x^{(2)} = \frac{\epsilon_{r,co}}{\epsilon_{r,co} n_y^2 + \epsilon_{r,cl} n_x^2} E_x^{(1)} + \frac{(\epsilon_{r,co} - \epsilon_{r,cl}) n_x n_y}{\epsilon_{r,co} n_y^2 + \epsilon_{r,cl} n_x^2} E_y^{(2)}. \quad (20)$$

$E_x^{(1)}$ and $E_y^{(2)}$ can be obtained by the linear interpolation and extrapolation of nearby fields, i.e.,

$$E_x^{(1)} = \left(\frac{3}{2} - \gamma_x\right) E_x, (k-1/2, \ell, m) - \left(\frac{1}{2} - \gamma_x\right) E_x, (k-3/2, \ell, m) \quad (21)$$

$$E_y^{(2)} = (1 + \gamma_x) \frac{E_y, (k, \ell+1/2, m) + E_y, (k, \ell-1/2, m)}{2} - \gamma_x \frac{E_y, (k+1, \ell+1/2, m) + E_y, (k+1, \ell-1/2, m)}{2}. \quad (22)$$

As a result, (17) is calculated using (20)–(22). The position of an arbitrary dielectric interface is set by γ_x , while the direction of a unit normal vector is set by n_x and n_y .

Following the same procedure for evaluating (17), we can obtain an FD formula for $\delta_x E_z, (k-1/2, \ell, m+1/2)$ in (7)

$$\delta_x E_z, (k-1/2, \ell, m+1/2) = \frac{1}{1 - \gamma_x} \frac{E_z^{(1)} - E_z, (k-1, \ell, m+1/2)}{\Delta x} \quad (23)$$

$$\begin{aligned} E_z^{(1)} &= E_z^{(2)} \\ &= (1 + \gamma_x) E_z, (k, \ell, m+1/2) \\ &\quad - \gamma_x E_z, (k+1, \ell, m+1/2). \end{aligned} \quad (24)$$

Furthermore, $\delta_x H_x, (k-1/2, \ell-1/2, m+1/2)$ in (12) and $\delta_x H_z, (k, \ell-1/2, m)$ in (9) are calculated with the use of the boundary conditions of $\mathbf{n} \times \mathbf{H}^{(1)} = \mathbf{n} \times \mathbf{H}^{(2)}$ and $\mathbf{n} \cdot \mu_r \mathbf{H}^{(1)} = \mathbf{n} \cdot \mu_r \mathbf{H}^{(2)}$. Recall that μ_r has been omitted due to a unit value. Hence, the treatments of the magnetic-field components are simplified in comparison with those of the electric-field components in (17), i.e.,

$$\begin{aligned} \delta_x H_x, (k-1/2, \ell-1/2, m+1/2) \\ &= \frac{1}{1 - \gamma_x} \frac{H_x^{(1)} - H_x, (k-1, \ell-1/2, m+1/2)}{\Delta x} \end{aligned} \quad (25)$$

$$\begin{aligned} H_x^{(1)} &= H_x^{(2)} \\ &= (1 + \gamma_x) H_x, (k, \ell-1/2, m+1/2) \\ &\quad - \gamma_x H_x, (k+1, \ell-1/2, m+1/2) \end{aligned} \quad (26)$$

$$\begin{aligned} \delta_x H_z, (k, \ell-1/2, m) \\ &= \frac{2}{1 + 2\gamma_x} \frac{H_z, (k+1/2, \ell-1/2, m) - H_z^{(2)}}{\Delta x} \end{aligned} \quad (27)$$

$$\begin{aligned} H_z^{(2)} &= H_z^{(1)} \\ &= \left(\frac{3}{2} - \gamma_x\right) H_z, (k-1/2, \ell-1/2, m) \\ &\quad - \left(\frac{1}{2} - \gamma_x\right) H_z, (k-3/2, \ell-1/2, m). \end{aligned} \quad (28)$$

The modified FD formula is also derived for the derivatives with respect to y . The formula for δ_y is used in combination with that for δ_x .

It should be noted that the modified FD formula slightly affects the stability criterion [15]. Although $\Delta\tau/\Delta t$ in the modified method has to be a smaller value than that in the conventional method, the modified method has high computational efficiency, as will be demonstrated in Section III.

C. Body-of-Revolution (BOR) Imaginary-Distance Propagation Method

The BOR technique [7] has often been employed for the FDTD analysis of axially symmetric optical elements [20], [21]. The use of the technique enables us to accurately describe the circular interface in the cylindrical coordinates based on Yee's mesh. We are, therefore, interested in investigating the extent to which the results obtained by the modified FD formula in rectangular coordinates coincide with those by the BOR technique. A BOR imaginary-distance propagation method can be formulated as follows.

Cylindrical and rectangular coordinates are related by $x = \rho \cos \phi$ and $y = \rho \sin \phi$. The electric and magnetic fields for the $\text{HE}_{\ell 1}$ mode ($\ell \geq 1$) are expressed as

$$\bar{\mathbf{E}}(\rho, \phi, z, t) = \mathbf{E}_{(\rho, z)} \exp(j\ell\phi) \exp[j(\omega t - \beta_{\text{ref}} z)] \quad (29)$$

$$\bar{\mathbf{H}}(\rho, \phi, z, t) = \mathbf{H}_{(\rho, z)} \exp(j\ell\phi) \exp[j(\omega t - \beta_{\text{ref}}z)] \quad (30)$$

where $\exp(j\ell\phi)$ represents the azimuthal dependence of the fields. Consequently, the partial derivative in ϕ is performed analytically [7], [20], [21]. This means that the BOR technique reduces the original three-dimensional model to an equivalent two-dimensional one.

Substituting (29) and (30) into Maxwell's equations in cylindrical coordinates, we obtain the following difference equations:

$$\begin{aligned} E_{\rho, (k+1/2, m+1)} &= \frac{1}{1 - j\beta_{\text{ref}}\Delta z/2} \times \left[(1 + j\beta_{\text{ref}}\Delta z/2)E_{\rho, (k+1/2, m)} \right. \\ &\quad + \Delta z \delta_{\rho} E_{z, (k+1/2, m+1/2)} \\ &\quad \left. - jk_0 \Delta z H_{\phi, (k+1/2, m+1/2)} \right] \quad (31) \end{aligned}$$

$$\begin{aligned} E_{\phi, (k, m+1)} &= \frac{1}{1 - j\beta_{\text{ref}}\Delta z/2} \times \left[(1 + j\beta_{\text{ref}}\Delta z/2)E_{\phi, (k, m)} \right. \\ &\quad + j \frac{\ell \Delta z}{\rho^{(k)}} E_{z, (k, m+1/2)} \\ &\quad \left. + jk_0 \Delta z H_{\rho, (k, m+1/2)} \right] \quad (32) \end{aligned}$$

$$\begin{aligned} H_{\rho, (k, m+1/2)} &= \frac{1}{1 - j\beta_{\text{ref}}\Delta z/2} \times \left[(1 + j\beta_{\text{ref}}\Delta z/2)H_{\rho, (k, m-1/2)} \right. \\ &\quad + \Delta z \delta_{\rho} H_{z, (k, m)} \\ &\quad \left. + jk_0 \Delta z \epsilon_{r, (k)} E_{\phi, (k, m)} \right] \quad (33) \end{aligned}$$

$$\begin{aligned} H_{\phi, (k+1/2, m+1/2)} &= \frac{1}{1 - j\beta_{\text{ref}}\Delta z/2} \times \left[(1 + j\beta_{\text{ref}}\Delta z/2)H_{\phi, (k+1/2, m-1/2)} \right. \\ &\quad + j \frac{\ell \Delta z}{\rho^{(k+1/2)}} H_{z, (k+1/2, m)} \\ &\quad - jk_0 \Delta z \epsilon_{r, (k+1/2)} \\ &\quad \left. \cdot E_{\rho, (k+1/2, m)} \right] \quad (34) \end{aligned}$$

$$\begin{aligned} E_{z, (k, m+1/2)} &= \frac{1}{(1 - j\beta_{\text{ref}}\Delta z/2)\epsilon_{r, (k)}} \\ &\times \left[(1 + j\beta_{\text{ref}}\Delta z/2)\epsilon_{r, (k)} \right. \\ &\quad \cdot E_{z, (k, m-1/2)} - \frac{\Delta z}{\rho^{(k)}} \delta_{\rho} \{ \rho^{(k)} \epsilon_{r, (k)} E_{\rho, (k, m)} \} \\ &\quad \left. - j \frac{\ell \Delta z}{\rho^{(k)}} \epsilon_{r, (k)} E_{\phi, (k, m)} \right] \quad (35) \end{aligned}$$

$$\begin{aligned} H_{z, (k+1/2, m+1)} &= \frac{1}{(1 - j\beta_{\text{ref}}\Delta z/2)} \\ &\times \left[(1 + j\beta_{\text{ref}}\Delta z/2)H_{z, (k+1/2, m)} \right. \\ &\quad - \frac{\Delta z}{\rho^{(k+1/2)}} \delta_{\rho} \{ \rho^{(k+1/2)} H_{\rho, (k+1/2, m+1/2)} \} \\ &\quad \left. - j \frac{\ell \Delta z}{\rho^{(k+1/2)}} H_{\phi, (k+1/2, m+1/2)} \right] \quad (36) \end{aligned}$$

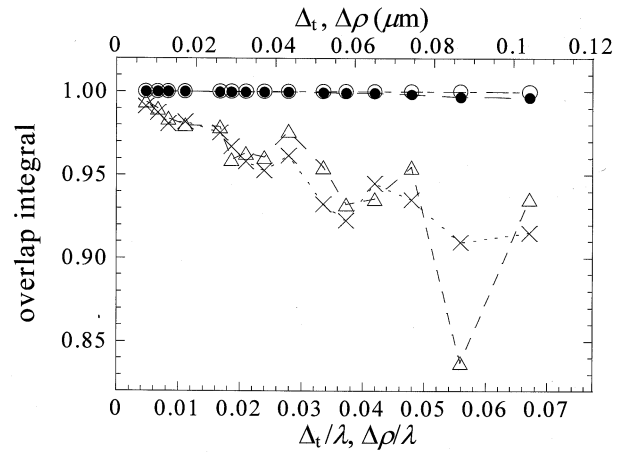


Fig. 2. Overlap integral as a function of Δt (minor component E_y). Modified FD formula \bullet , staircase approximation \times , EDCT \triangle , and BOR technique \circ .

where $(k\Delta\rho, m\Delta z) = (\rho, z)$ and δ_{ρ} is a difference operator. It should be noted that (31)–(36) can be utilized for the computations of field components away from the z -axis.

The field components on the z -axis, $E_z, (k=0)$, $E_{\phi, (k=0)}$, and $H_{\rho, (k=0)}$, are treated as follows [7], [20], [21]: $E_z, (k=0)$ for the $\text{HE}_{\ell p}$ mode can be obtained by Ampere's law of

$$\iint_S \frac{\epsilon_r}{c_0} \frac{\partial}{\partial t} \bar{\mathbf{E}} dS = \oint_l \bar{\mathbf{H}} dl$$

i.e.,

$$\begin{aligned} jk_0 \epsilon_{r, (k=0)} E_{z, (k=0)} \pi \left(\frac{\Delta\rho}{2} \right)^2 \\ = \int_0^{2\pi} H_{\phi, (k=1/2)} \exp(j\ell\phi) \frac{\Delta\rho}{2} d\phi = 0. \quad (37) \end{aligned}$$

Thus, $E_z, (k=0)$ is fixed to be zero. Fortunately, we can omit $H_{\rho, (k=0)}$, since $H_{\rho, (k=0)}$ is multiplied by the factor $\rho^{(k=0)} = 0$ in (36). As a result, $E_{\phi, (k=0)}$ is not needed to evaluate the relevant fields [$E_z, (k=0)$ and $H_{\rho, (k=0)}$], so that $E_{\phi, (k=0)}$ is also omitted.

In the BOR technique, the E_z , E_{ϕ} , and H_{ρ} components can be placed on a dielectric interface. E_z and E_{ϕ} are tangential to the interface, while H_{ρ} is vertical, so that the fields are continuous at the interface. For this case, δ_{ρ} can be approximated by the central-difference operator, and interface conditions can be determined by Ampere's and Faraday's laws [7]. We estimate that $\epsilon_{r, (k)}$ on the interface equals the average of the relative permittivities along the interface [5].

Finally, the BOR imaginary-distance propagation method is obtained by changing the coordinate z in the propagation direction to $j\tau$. The derived method is applied to the evaluation of the fundamental mode (HE_{11}) in the next section. (This method can also give higher order modes, such as HE_{21} and HE_{31} , without using a special technique [4].)

III. RESULTS

We assess the accuracy of the modified method in the analysis of the HE_{11} mode of a step-index circular fiber. The refractive indexes of the core and cladding are chosen to be $\sqrt{\epsilon_{r, \text{co}}} = 1.5$ and $\sqrt{\epsilon_{r, \text{cl}}} = 1$, respectively. A wavelength of $\lambda = 1.55 \mu\text{m}$

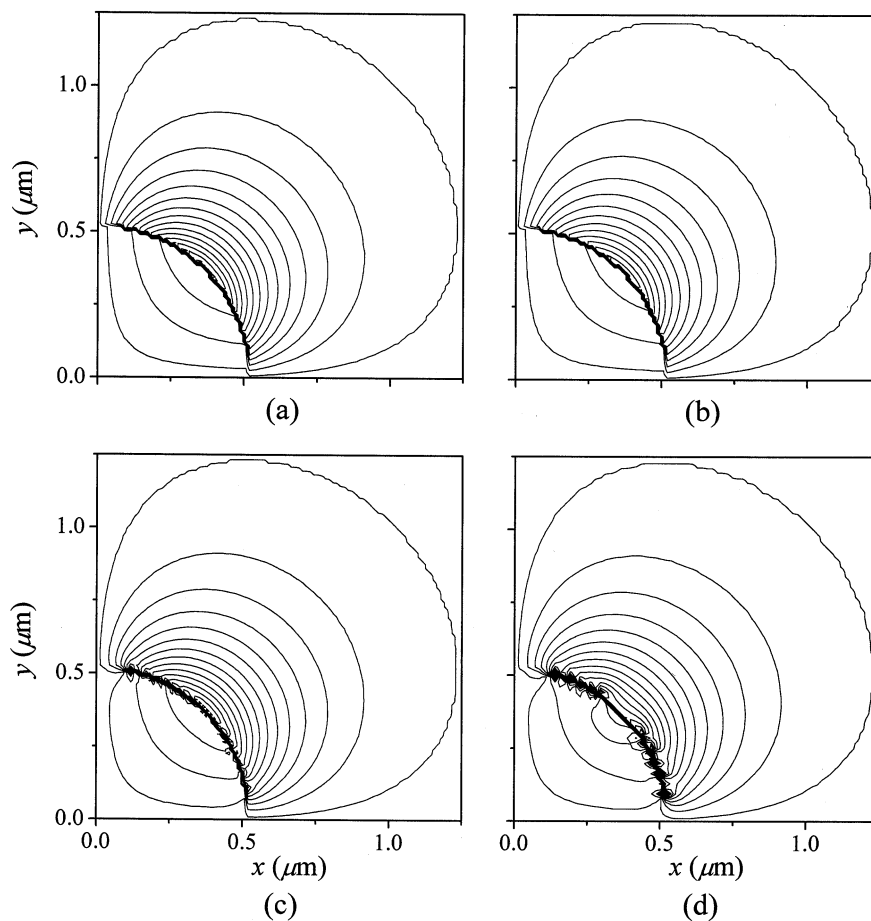


Fig. 3. Field distribution of minor component E_y for $\Delta_t = 0.0084\lambda$ (quarter region). (a) Modified FD formula. (b) Exact solutions. (c) EDCT. (d) Staircase approximation.

and a core radius of $R = 0.52 \mu\text{m}$ are used, so that the normalized frequency is $V \cong 2.36$. This fiber is not realistic, but is considered to investigate the sensitivity of the modified method in a strongly guiding structure. (We also analyzed a fiber with a higher value of permittivity, i.e., $\sqrt{\epsilon_{r,\text{co}}} = 3.6$, and confirmed that the effects of the modified method are essentially the same as those to be presented in Figs. 2 and 4.) The computational domain is fixed to be $L_x \times L_y = 5.2 \mu\text{m} \times 5.2 \mu\text{m}$. The transverse mesh size is designated as $\Delta_t (= \Delta x = \Delta y)$.

Consideration is given to the accuracy of the field profile. Fig. 2 shows the overlap integral between the numerical and exact field profiles of the minor component E_y as a function of Δ_t . For comparison, we present the data obtained by other techniques, i.e., the staircase approximation and the typical EDCT [12] that has recently been proposed. It is clearly seen that the modified method leads to substantial improvement in accuracy over other techniques. Although not plotted, a similar tendency is observed in all electric- and magnetic-field components.

Fig. 2 also presents the data evaluated by the BOR imaginary-distance propagation method. Note that we can obtain the field profile of E_y by the vector transformation from cylindrical-to-rectangular [22, Appendix II]. Since the BOR technique accurately describes the circular interface, the discretization error is eliminated without modifying the FD equations. As

can be seen, the data calculated by the modified FD formula are in agreement with those by the BOR technique.

Fig. 3 illustrates the typical contour plots of the E_y components for $\Delta_t = 0.0084\lambda (= R/40)$ evaluated by four methods. The field distribution obtained by the modified method [Fig. 3(a)] remarkably agrees with that by the exact solution [Fig. 3(b)]. On the other hand, the EDCT [Fig. 3(c)] cannot sufficiently eliminate the numerical noise around the core-cladding interface caused by the staircase approximation [Fig. 3(d)]. It can be said that the modified FD formula greatly contributes to a reduction in the discretization error.

The accuracy of the modified method is also assessed by the evaluation of the propagation constant. In the imaginary-distance procedure, the propagation constant of the eigenmode β_0 can be obtained by the growth ($\beta_0 > \beta_{\text{ref}}$) or decay ($\beta_0 < \beta_{\text{ref}}$) in the propagating field amplitude at τ and $\tau + \Delta\tau$ [2], [4]

$$\beta(\tau) = \beta_{\text{ref}} + \lim_{\tau \rightarrow \infty} \frac{\iint_S [\ln\{\varphi(\tau + \Delta\tau)\} - \ln\{\varphi(\tau)\}] |\varphi(\tau)|^2 dS}{\Delta\tau \iint_S |\varphi(\tau)|^2 dS} \equiv \beta_0 \quad (38)$$

where the weighted average is introduced to minimize numerical errors [4]. For the calculation of β_0 using (38), we employ a technique for iteratively renewing β_{ref} [23].

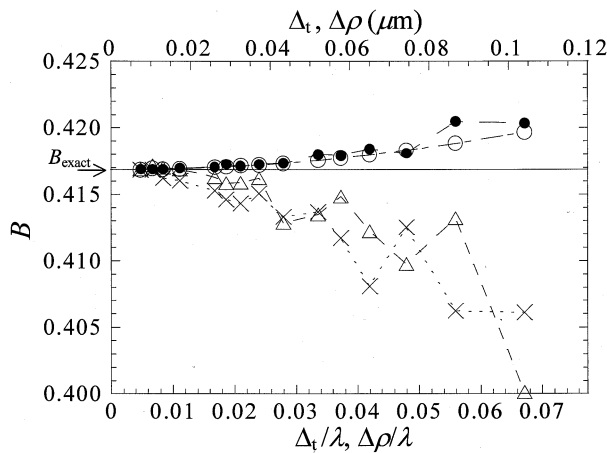


Fig. 4. Normalized propagation constant B as a function of Δ_t . Modified FD formula \bullet , staircase approximation \times , EDCT \triangle , and BOR technique \circ .

TABLE I
COMPUTATIONAL EFFICIENCY

Method	Δ_t/λ	$\Delta\tau/\lambda$	Propa- gation steps	CPU time (s)	Mem- ory (MB)
Modified	0.037	0.018	300	55	2.7
EDCT	0.037	0.025	212	31	2.3
	0.024	0.016	362	126	4.3
	0.0065	0.0043	1222	5450	44

The effective relative permittivity is defined as $\epsilon_{r,\text{eff}} = (\beta_0/k_0)^2$, and the normalized propagation constant is $B = (\epsilon_{r,\text{eff}} - \epsilon_{r,\text{cl}})/(\epsilon_{r,\text{co}} - \epsilon_{r,\text{cl}})$. Convergence behavior of B as a function of Δ_t is shown in Fig. 4. It is worth mentioning that the modified FD formula achieves faster convergence than the staircase approximation and EDCT. Note that the BOR technique leads to monotone convergence to the exact value B_{exact} . The convergence behavior of the modified FD formula is almost similar to that of the BOR technique. This suggests that the modified FD formula exactly evaluates the behavior of the field vectors across an arbitrary interface in rectangular coordinates.

The computational efficiency of the modified method is another topic of interest. Table I tabulates CPU time and memories, in which the convergence of B in six decimal places is obtained. The calculations are performed on a Pentium 800-MHz PC. For reference, the data of the EDCT are also presented for three values of Δ_t . Recall that $\Delta\tau/\Delta_t$ has to be a value for which the scheme becomes numerically stable. For this investigation, $\Delta\tau$ is chosen to be a maximum value within the stability criterion. When Δ_t is chosen to be $0.037\lambda (=R/9)$ in the modified method, $|B - B_{\text{exact}}|$ is evaluated to be less than 0.001 (Fig. 4), while the overlap integral is evaluated to be greater than 0.999 (Fig. 2). Table I shows that the modified method needs more CPU time and memories in comparison with the EDCT for $\Delta_t = 0.037\lambda$. However, the EDCT requires that Δ_t be re-

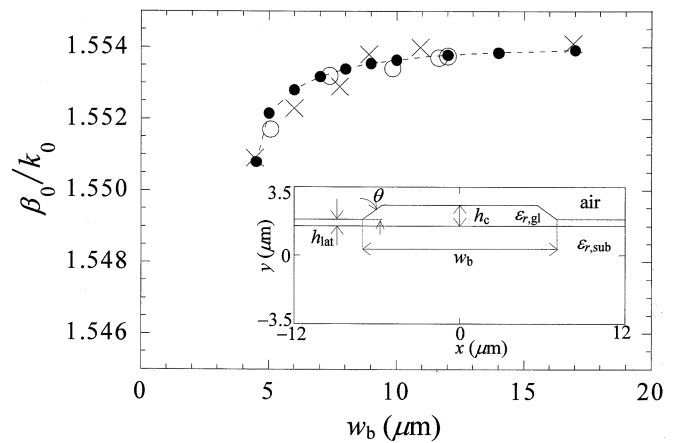


Fig. 5. Effective index β_0/k_0 as a function of w_b (E_{11}^x mode). Modified FD formula \bullet , theoretical [23] \circ , and experimental [23] \times .

duced to $0.024\lambda (=R/14)$ so as to obtain $|B - B_{\text{exact}}| < 0.001$. Furthermore, to obtain an overlap integral of greater than 0.99 by the EDCT, we have to reduce Δ_t to $0.0065\lambda (=R/52)$. Consequently, it can be said that the use of the modified FD formula reduces the CPU time and memories while maintaining comparable accuracy.

We finally treat the sloped-side rib guide [19] illustrated in the inset of Fig. 5. The configuration parameters are $\sqrt{\epsilon_{r,\text{sub}}} = 1.538$, $\sqrt{\epsilon_{r,\text{gl}}} = 1.568$, $\lambda = 0.633 \mu\text{m}$, sidewall angle $\theta = 32^\circ$, central rib height $h_c = 1.07 \mu\text{m}$, lateral height $h_{\text{lat}} = 0.34 \mu\text{m}$, and base width of the rib w_b , varying from 4.5 to $17 \mu\text{m}$. The transverse mesh size is fixed to be $\Delta_t = 0.025 \mu\text{m} (=0.039\lambda)$.

Fig. 5 shows the effective index β_0/k_0 as a function of w_b , where β_0 is the propagation constant of the E_{11}^x mode. The data presented by open circles and crosses are the calculated and experimental results presented in [19], respectively. The values of β_0/k_0 evaluated by the modified method agree well with the previously published data. We also show the typical contour plots of E_x and E_y for $w_b = 10 \mu\text{m}$ in Fig. 6. The electric field discontinuities across the sloped side and the horizontal interfaces are clearly observed in E_y [Fig. 6(b)].

IV. CONCLUSION

We have applied a modified FD formula that takes into account the boundary conditions at a dielectric interface to an imaginary-distance propagation method based on Yee's mesh. To demonstrate the validity of the modified method, we have analyzed the eigenmode of a step-index circular fiber. Calculations of the field profiles show that the modified FD formula greatly contributes to a reduction in a discretization error. In the evaluation of the normalized propagation constant against transverse mesh size, the modified FD formula achieves faster convergence than a staircase approximation and an effective-dielectric-constant technique. It is revealed that the results obtained by the modified FD formula coincide with those by a body-of-revolution technique, which accurately describes the circular interface. As a further application, we have evaluated the eigenmodes of sloped-side rib guides. The obtained data agree well with previously published data including calculated and experimental results.

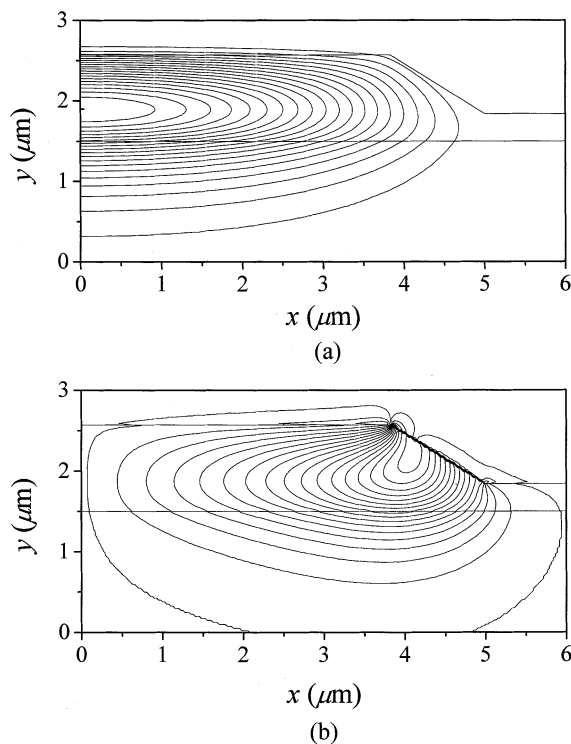


Fig. 6. Field distributions for $w_b = 10 \mu\text{m}$ (half region). (a) Major component E_x . (b) Minor component E_y .

ACKNOWLEDGMENT

The authors would like to thank Dr. A. Ditkowski and Dr. C. H. Teng of Brown University for sending [15] and [17] regarding the modified finite-difference formula.

REFERENCES

[1] M. Koshiba, *Optical Waveguide Analysis*. New York: McGraw-Hill, 1990.
 [2] D. Yevick and W. Bardyszewski, "Correspondence of variation finite-difference (relaxation) and imaginary-distance propagation methods for modal analysis," *Opt. Lett.*, vol. 17, no. 5, pp. 329–330, 1992.
 [3] C. Vassallo, "1993–1995 Optical mode solvers," *Opt. Quantum Electron.*, vol. 29, pp. 95–114, 1997.
 [4] S. M. Lee, "Finite-difference vectorial-beam-propagation method using Yee's discretization scheme for modal fields," *J. Opt. Soc. Amer. A*, vol. 13, no. 7, pp. 1369–1377, 1996.
 [5] J. Yamauchi, N. Morohashi, and H. Nakano, "Rib waveguide analysis by the imaginary-distance beam-propagation method based on Yee's mesh," *Opt. Quantum Electron.*, vol. 30, pp. 397–401, 1998.
 [6] T. Ando, J. Yamauchi, and H. Nakano, "Rectangular dielectric-rod fed by a metallic waveguide," *Proc. Inst. Elect. Eng. Microwave Antennas Propagat.*, 2002, to be published.
 [7] A. Taflove and S. C. Hagness, *Computational Electrodynamics, The Finite-Difference Time-Domain Method*, 2nd ed. Norwood, MA: Artech House, 2000.
 [8] T. G. Jurgens, A. Taflove, K. Umashankar, and T. G. Moore, "Finite-difference time-domain modeling of curved surfaces," *IEEE Trans. Antennas Propagat.*, vol. 40, no. 4, pp. 357–365, 1992.
 [9] M. C. Marcysiak and W. K. Gwarek, "Higher-order modeling of media interfaces for enhanced FDTD analysis of microwave circuits," in *Proc. 24th Eur. Microwave Conf.*, Cannes, France, 1994, pp. 1530–1535.
 [10] N. Kaneda, B. Houshmand, and T. Itoh, "FDTD analysis of dielectric resonators with curved surfaces," *IEEE Trans. Microwave Theory Tech.*, vol. 45, no. 9, pp. 1645–1649, 1997.

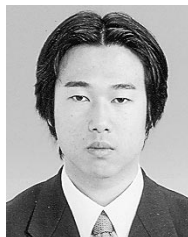
[11] G. Marrocco, M. Sabbadini, and F. Bardati, "FDTD improvement by dielectric subgrid resolution," *IEEE Trans. Microwave Theory Tech.*, vol. 46, no. 12, pp. 2166–2169, 1998.
 [12] W. Yu and R. Mittra, "A conformal finite difference time domain technique for modeling curved dielectric surfaces," *IEEE Microwave Wireless Components Lett.*, vol. 11, no. 1, pp. 25–27, 2001.
 [13] T. Hirono, Y. Shibata, W. W. Lui, S. Seki, and Y. Yoshikuni, "The second-order condition for the dielectric interface orthogonal to the Yee-lattice axis in the FDTD scheme," *IEEE Microwave Guided Wave Lett.*, vol. 10, no. 9, pp. 359–361, 2000.
 [14] K. H. Dridi and J. S. Hesthaven, " N -space stair case-free finite-difference time-domain formulation for arbitrary material distributions: Numerical investigations of a focusing grating coupler in dielectric waveguides," in *OSA Integr. Photon. Res. Dig.*, 1999, pp. 250–252.
 [15] A. Ditkowski, K. Dridi, and J. S. Hesthaven, "Convergent Cartesian grid methods for Maxwell's equations in complex geometries," *J. Comput. Phys.*, vol. 170, no. 4, pp. 39–80, 2001.
 [16] K. H. Dridi, J. S. Hesthaven, and A. Ditkowski, "Staircase-free finite-difference time-domain formulation for general materials in complex geometries," *IEEE Trans. Antennas Propagat.*, vol. 49, no. 5, pp. 749–756, 2001.
 [17] C. H. Teng, A. Ditkowski, and J. S. Hesthaven, "Modeling dielectric interfaces in the FDTD-method: A comparative study," submitted for publication.
 [18] T. Ando, H. Nakayama, J. Yamauchi, and H. Nakano, "Application of a modified finite-difference formula based on Yee's mesh to optical waveguide analyses," in *OSA Integr. Photon. Res. Dig.*, 2001, pp. ITuF4-1–ITuF4-3.
 [19] P. M. Pelosi, P. Vandenbulcke, C. D. W. Wilkinson, and R. M. D. L. Rue, "Propagation characteristics of trapezoidal cross-section ridge optical waveguides: An experimental and theoretical investigation," *Appl. Opt.*, vol. 17, no. 8, pp. 1187–1193, 1978.
 [20] D. B. Davidson and R. W. Ziolkowski, "Body-of-revolution finite-difference time-domain modeling of space-time focusing by a three-dimensional lens," *J. Opt. Soc. Amer. A*, vol. 11, no. 4, pp. 1471–1490, 1994.
 [21] D. W. Prather and S. Shi, "Formulation and application of the finite-difference time-domain method for the analysis of axially symmetric diffractive optical elements," *J. Opt. Soc. Amer. A*, vol. 16, no. 5, pp. 1131–1142, 1999.
 [22] C. A. Balanis, *Advanced Engineering Electromagnetics*. New York: Wiley, 1989.
 [23] J. Yamauchi, G. Takahashi, and H. Nakano, "Full-vectorial beam-propagation method based on the McKee–Mitchell scheme with improved finite-difference formulas," *J. Lightwave Technol.*, vol. 16, no. 12, pp. 2458–2464, 1998.



Takashi Ando (S'99) was born in Ibaraki, Japan, on March 14, 1969. He received the B.E. and M.E. degrees from Hosei University, Tokyo, Japan, in 1991 and 1993, respectively, where he is currently pursuing the Dr.E. degree.

From 1993 to 1998, he was with TDK Corporation, Tokyo. His research interests include optical waveguides and dielectric antennas.

Mr. Ando is a Member of the Institute of Electronics, Information and Communication Engineers (IEICE) of Japan.



Hiroki Nakayama was born in Kanagawa, Japan, on February 15, 1977. He received the B.E. degree from Hosei University, Tokyo, Japan, in 2000, where he is currently pursuing the M.E. degree.

His research interests include numerical analysis of optical waveguides.

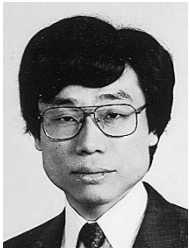
Mr. Nakayama is a Member of the Institute of Electronics, Information and Communication Engineers (IEICE) of Japan.



Satoshi Numata was born in Kanagawa, Japan, on May 27, 1977. He received the B.E. degree from Hosei University, Tokyo, Japan, in 2000, where he is currently pursuing the M.E. degree.

His research interests include numerical analysis of dielectric waveguides.

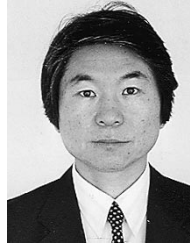
Mr. Numata is a Member of the Institute of Electronics, Information and Communication Engineers (IEICE) of Japan.



Junji Yamauchi (M'85) was born in Nagoya, Japan, on August 23, 1953. He received the B.E., M.E., and Dr.E. degrees from Hosei University, Tokyo, Japan, in 1976, 1978, and 1982, respectively.

From 1984 to 1988, he was a Lecturer in the Electrical Engineering Department, Tokyo Metropolitan Technical College. Since 1988, he has been a Member of the Faculty of Hosei University, where he is now a Professor of electronic informatics. His research interests include optical waveguides and circularly polarized antennas.

Dr. Yamauchi is a Member of the Optical Society of America and the Institute of Electronics, Information and Communication Engineers (IEICE) of Japan.



Hisamatsu Nakano (M'75–SM'87–F'92) was born in Ibaraki, Japan, on April 13, 1945. He received the B.E., M.E., and Dr.E. degrees in electrical engineering from Hosei University, Tokyo, Japan, in 1968, 1970, and 1974, respectively.

Since 1973, he has been a Member of the Faculty of Hosei University, where he is now a Professor of electronic informatics. His research topics include numerical methods for antennas, electromagnetic wave scattering problems, and light wave problems.

He has published more than 160 refereed journal papers and 120 international symposium papers on antenna and relevant problems. He is the author of *Helical and Spiral Antennas* (New York: Research Studies Press/Wiley, 1987). He published the chapter "Antenna Analysis Using Integral Equations" in *Analysis Methods of Electromagnetic Wave Problems*, vol. 2 (Norwood, MA: Artech House, 1996). He was a Visiting Associate Professor at Syracuse University, Syracuse, NY, during May–September 1981, a Visiting Professor at the University of Manitoba, Canada, during March–September 1986, and a Visiting Professor at the University of California, Los Angeles, during September 1986–March 1987.

Dr. Nakano received an International Scientific Exchange Award from the Natural Sciences and Engineering Research Council of Canada. In 1987, he received the Best Paper Award from the Institute of Electrical Engineering 5th International Conference on Antennas and Propagation. In 1994, he received the IEEE AP-S Best Application Paper Award (H. A. Wheeler Award). He is an Associate Editor of IEEE ANTENNAS AND PROPAGATION MAGAZINE. He is a Member of the AP-S Administrative Committee in 2002.